Bonding in phosphorus ylides: topological analysis of experimental charge density distribution in triphenylphosphonium benzylide †

Dmitrii S. Yufit,* Judith A. K. Howard and Matthew G. Davidson

Department of Chemistry, University of Durham, Durham, UK DH1 3LE

Received (in Cambridge, UK) 8th October 1999, Accepted 22nd November 1999

The topological analysis of the experimentally determined charge density distribution in the semi-stabilized ylide Ph_3PCHPh revealed the multiple character and high ionicity of the ylide bond and a different role of the phenyl groups in charge delocalisation in the PPh_3 fragment. The analysis of intra- and inter-molecular contacts located the interactions which are responsible for the conformation of the molecule and determine the packing of the molecules in the crystal.

It is difficult to overestimate the importance of phosphorus ylides in synthetic organic chemistry. The nature of the $P–C_{ylide}$ bond is the main point of interest and became the subject of a great number of intensive debates based on the experimental data and theoretical calculations at different levels (see, for example, the comprehensive review[1] and references therein). The studies revealed that the bond is highly polar and has multiple character. A large variety of X-ray structures of ylides has been determined. In spite of all the attention, there are very few examples of experimental studies of electronic distribution in hypervalent phosphorus compounds and in ylides in particular. We are aware only of one experimental charge density study of a phosphonium ylide, namely triphenylphosphonium methylide.[2] This compound represents so-called non-stabilized ylides which have a pyramidal configuration of the ylide carbon atom. The study found an unexpected shift of the maximum of electron density on the $P–C_{ylide}$ bond out of the internuclear vector connecting the two atoms. The study has been performed using the X–X′ technique, which is rather qualitative and provides very useful, but limited information about charge density distribution in the molecules. However, much more information may be obtained from experimental high-resolution X-ray data using the multipole models and topological analysis of the electron distribution according to Bader's theory of "atoms in molecules" (AIM).[3] This approach can provide a new insight into the nature of bonding in phosphorus ylides and gives a useful reference point for the numerous theoretical calculations. In this paper we present the results of such a study for a semi-stabilised ylide—triphenylphosphonium benzylide, Ph_3PCHPh (**1**). The conventional X-ray structure of **1** has been published previously[4] and in that paper, special attention was paid to C–H···C intermolecular contacts which allegedly determine the crystal packing. Recently a number of successful studies of intermolecular interactions using AIM-analysis has been reported (see, for example, ref. 5) and the experimental confirmation of the existence of these contacts in the structure of **1** was another aim of our work.

Experimental

The synthesis of **1** has been described previously.[4] A pale red crystal ($0.16 \times 0.2 \times 0.56$ mm^3) of **1** was picked up under N_2 atmosphere from the mother solution, mounted on a glass fibre with an epoxy resin and immediately put on the goniometer under the stream of cold nitrogen gas from an *Oxford Cryostream* LT-device. Some details of data collection and refinement are given in Table 1. The face plate of the Bruker SMART CCD-detector was positioned at 3.5 cm from the optical centre of the goniometer. Measurements were made with two positions of the detector at $\theta = -32$ and $-75°$; with 4 and 5 positions of the φ-axis and 30 and 45 s. exposure respectively. A total of 6595 frames were collected using graphite monochromated Mo-Kα radiation and ω-scan mode (0.2°/frame). The data were processed with SAINT.[6] A number of routines for data processing were examined with variation of SAINT parameters for peak integration and consecutive application of different types of absorption correction and/or data merging using the SORTAV program of the DREAD package.[7] The best results, which are reported in the paper, were obtained using the separate processing of high- and low-order data with blending of the model profiles from different detector regions for high-order data. A total of 99436 reflections with $(\sin\theta/\lambda)_{max} \leq 1.14$ were processed yielding 22695 independent reflections with relatively modest $R_{int} = 0.0453$ due to the large number of data. For the 10427 independent reflections with $I \geq 2\sigma(I)$ the value of R_{int} is 0.0319. The absorption correction ($\mu = 0.15$ mm^{-1}) did not provide any noticeable improvement of the results and was not applied. The obtained data set was used for multipole refinement with the XD program package.

The rigid pseudo atom model implemented in XD is well-established and its detailed description can be found in a number of papers (see, for example, ref. 9). For carbon atoms

Table 1 Some experimental details for Ph_3PCHPh

Crystal data	
Chemical formula	$C_{25}H_{21}P$
Formula weight	352.9
Space group	$P2_1/c$, $Z = 4$
T/K	100
a/Å	9.397(1)
b/Å	10.968(1)
c/Å	18.397(1)
β/°	91.52(1)
V/Å^3	1895.8(1)
μ/mm^{-1}	0.15
R_{int} (for $I \geq 2\sigma(I)$)	0.032
R (10024 refl., $I \geq 2.5\sigma(I)$)	0.022
R_w	0.017
GOOF	0.72
No. of parameters	709

† Tables of atomic coordinates and anisotropic displacement parameters for compound **1**, multipole population coefficients, local co-ordination system, atomic charges and residual maps are available as supplementary data. For direct electronic access see http://www.rsc.org/suppdata/p2/a9/a908099f, otherwise available from BLDSC (SUPPL. NO. 57688, 10 pp.) or the RSC Library. See Instructions for Authors available *via* the RSC web page (http://www.rsc.org/authors).

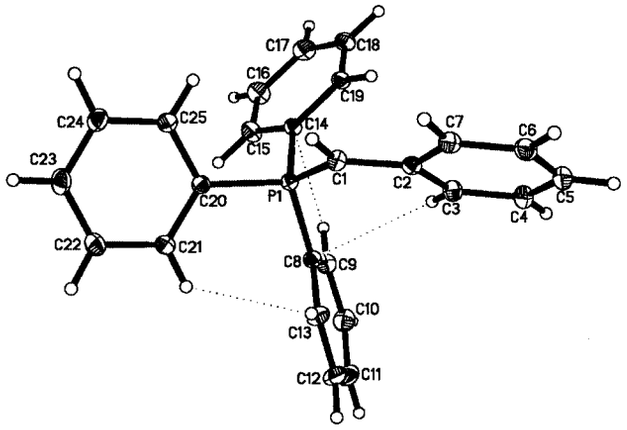

Fig. 1 General view of molecule **1** and the labeling scheme. Close intramolecular contacts are shown by dotted lines.

the multipole expansion has been applied up to octupole level ($l_{max} = 3$), for atom P the hexadecapoles ($l_{max} = 4$) were also refined. Only bond-directed dipoles ($l_{max} = 1$) were refined for H atoms. Hydrogen atoms were fixed at average neutronographic distances 1.083 Å (for C(1)–H(1) 1.080 Å)[10] from the parent carbon atoms and their positions were adjusted after each cycle of refinement. The directions of the C–H bonds and the isotropic atomic displacement parameters of the hydrogen atoms were taken from the spherical atom refinement and were not refined. It was found before[11] that the "standard" XD parameters of radial functions for 4-coordinated P atom are not optimal. In case of the molecule **1** the best results of the refinement (with flat featureless residual maps and extreme values of residual density of ±0.14 e Å^{-3}) were obtained with $n = 4,4,7,8,8$ for the phosphorus atom. The expansion-contraction coefficients κ' for P atom were refined independently for each level of multipoles; for C atoms the common κ' values were used for $l = 1$–3. The final model is consistent with rigid-body hypothesis: Hirshfeld's values[12] are less than 0.0008 Å^2. Tables of the atomic coordinates, the anisotropic displacement parameters, the multipole population coefficients, the local coordination system, the atomic charges as well as residual maps are submitted as Supplementary data. CCDC reference number 188/209. See http://www.rsc.org/suppdata/p2/a9/a908099f for crystallographic files in .cif format.

Results and discussion

The general view of the molecule **1** and the labeling scheme are shown in Fig. 1, geometrical parameters are given in Table 2. The molecular parameters correspond well to those reported in ref. 4 and are common for semi-stabilized and stabilized ylides. The ylide carbon atom, C(1), is planar. The phosphorus atom has the usual tetrahedral configuration with the longest P–C_{Ph} bond oriented almost perpendicular to the ylide plane (torsion angle C(2)C(1)PC(14) −75.5°), the shortest one is located almost in the ylide plane (torsion angle C(2)C(1)PC(20) 166.5°) and the intermediate one in the intermediate position (torsion angle C(2)C(1)PC(8) 46.0°). The bond angles at P atom decrease accordingly: C(14)PC(1) > C(8)PC(1) > C(20)PC(1). The *ipso*-bond angle C(3)C(2)C(7) is considerably decreased to 116.0° reflecting the electron-donor character of ylide carbon atom C(1).

Some maps of the Laplacian of electron density distribution are shown in Fig. 2, parameters of bond critical points (BCP) are given in Table 3. The values of total density, ρ, Laplacian and ellipticity in the BCP of C–C and C–H bonds in aromatic rings correspond well to those known for benzene,[13] supporting the credibility of model obtained. All BCP of P–C bonds have negative Laplacian values, which indicate the shared interactions and are usual for covalent bonds. On the other hand the

Table 2 Geometrical parameters of molecule **1** (Å, °)

P(1)–C(1)	1.6993(5)	C(11)–C(12)	1.3944(7)
P(1)–C(8)	1.8173(4)	C(12)–C(13)	1.3954(6)
P(1)–C(14)	1.8216(4)	C(14)–C(15)	1.4025(6)
P(1)–C(20)	1.8056(6)	C(14)–C(19)	1.3972(5)
C(1)–C(2)	1.4429(5)	C(15)–C(16)	1.3954(6)
C(2)–C(3)	1.4186(5)	C(16)–C(17)	1.3971(7)
C(2)–C(7)	1.4195(5)	C(17)–C(18)	1.3929(7)
C(3)–C(4)	1.3932(6)	C(18)–C(19)	1.3948(5)
C(4)–C(5)	1.3965(7)	C(20)–C(21)	1.3994(5)
C(5)–C(6)	1.3973(7)	C(20)–C(25)	1.4009(5)
C(6)–C(7)	1.3923(6)	C(21)–C(22)	1.3959(6)
C(8)–C(9)	1.4005(6)	C(22)–C(23)	1.3972(7)
C(8)–C(13)	1.4017(6)	C(23)–C(24)	1.3956(7)
C(9)–C(10)	1.3966(6)	C(24)–C(25)	1.3941(5)
C(10)–C(11)	1.3903(8)		
C(1)–P(1)–C(8)	113.2(1)	C(9)–C(10)–C(11)	120.1(1)
C(1)–P(1)–C(14)	116.7(1)	C(10)–C(11)–C(12)	120.3(1)
C(1)–P(1)–C(20)	107.1(1)	C(11)–C(12)–C(13)	119.7(1)
C(8)–P(1)–C(14)	104.6(1)	C(8)–C(13)–C(12)	120.3(1)
C(8)–P(1)–C(20)	109.3(1)	P(1)–C(14)–C(15)	122.8(1)
C(14)–P(1)–C(20)	105.5(1)	P(1)–C(14)–C(19)	117.6(1)
P(1)–C(1)–C(2)	127.0(1)	C(15)–C(14)–C(19)	119.6(1)
P(1)–C(1)–H(1)	115.1(1)	C(14)–C(15)–C(16)	120.0(1)
C(2)–C(1)–H(1)	117.6(1)	C(15)–C(16)–C(17)	120.0(1)
C(1)–C(2)–C(3)	124.2(1)	C(16)–C(17)–C(18)	120.2(1)
C(1)–C(2)–C(7)	119.8(1)	C(17)–C(18)–C(19)	119.9(1)
C(3)–C(2)–C(7)	116.0(1)	C(14)–C(19)–C(18)	120.4(1)
C(2)–C(3)–C(4)	121.8(1)	P(1)–C(20)–C(21)	122.8(1)
C(3)–C(4)–C(5)	121.1(1)	P(1)–C(20)–C(25)	117.2(1)
C(4)–C(5)–C(6)	118.2(1)	C(21)–C(20)–C(25)	119.8(1)
C(5)–C(6)–C(7)	121.1(1)	C(20)–C(21)–C(22)	119.9(1)
C(2)–C(7)–C(6)	121.8(1)	C(21)–C(22)–C(23)	120.0(1)
P(1)–C(8)–C(9)	122.7(1)	C(22)–C(23)–C(24)	120.2(1)
P(1)–C(8)–C(13)	117.8(1)	C(23)–C(24)–C(25)	119.8(1)
C(9)–C(8)–C(13)	119.4(1)	C(20)–C(25)–C(24)	120.2(1)
C(8)–C(9)–C(10)	120.0(1)		

ylide bond is very polar: atomic charges (calculated as a difference between monopole population and a number of valent electrons) for P and C(1) are +0.49 and −0.41 respectively. A particularly noteworthy feature of molecule **1** is a very high ellipticity of the ylide bond P–C(1) and also of the C(1)–C(2) bond. It implies the particular multiple character of these bonds and a high degree of delocalisation over the P–C(1)–Ph system. The Laplacian distribution of the P–C(1) and P–C(14) bonds is distinctively asymmetric (Fig. 2), with a shift of the charge concentration towards the area of σ*-orbitals of the P–C bonds. It is not the case for the other two P–Ph bonds (Fig. 2). All these observations are in good agreement with the results of DFT-calculations of trimethylphosphonium methylide,[14] which show the presence of one π-back donation interaction from the non-bonding *p* orbital of the ylide carbon atom. There is no significant deviation of the position of the BCP of the ylide bond in molecule **1** away from the corresponding internuclear vector as was found in triphenylphosphonium methylide.[2] One of the possible reasons for this dissimilarity could be the difference in electronic structures of non-stabilised and semi-stabilised ylides, due to the pyramidal configuration of the ylide carbon atom in the former ones.

Further analysis of the positions of the BCP can provide useful information about the fine electronic structure of the molecule.[15] The positions of BCP's in the P–C(1)–C(2) system of molecule **1** are rather unusual. In the case of different atomic charges of the covalently bonded atoms one can expect to observe the shift of the BCP towards the more positive atom, which reflects the accumulation of electron density in the atomic basin of the more negative atom. In molecule **1** the pronounced shift of the BCP positions towards the positively charged phosphorus atom is observed for the P–C(1) and P–C(8) bonds (see Table 3). However, for the P–C(20) and P–C(14) bonds, as well as for the C(1)–C(2) bond, a shift in the opposite

Table 3 Parameters of the BCP for the bonds between non-hydrogen atoms in molecule **1** (ρ/e Å^{-3}, total electron density; $\nabla^2(\rho)$/e Å^{-5}, Laplacian; λ_1, λ_2, λ_3, eigenvalues of Hessian matrix; ε, ellipticity; $\Delta_{ij} = (d_1 - d_2)/(d_1 + d_2)$, where d_1 and d_2 are distances along bond paths from the BCP to the first and second bonded atoms respectively)

Bond	ρ	$\nabla^2(\rho)$	λ_1	λ_2	λ_3	ε	Δ_{ij}
P(1)–C(1)	1.45(1)	−10.56(4)	−8.83	−5.86	4.13	0.51	−0.053
P(1)–C(8)	1.217(9)	−9.12(4)	−6.41	−6.35	3.64	0.01	−0.059
P(1)–C(14)	1.347(8)	−9.34(3)	−7.83	−7.27	5.77	0.08	0.021
P(1)–C(20)	1.364(9)	−12.05(3)	−8.30	−7.84	4.09	0.06	0.018
C(1)–C(2)	1.910(9)	−13.65(2)	−13.09	−10.82	10.26	0.21	−0.012
C(2)–C(3)	2.090(9)	−17.55(2)	−14.31	−12.72	9.48	0.13	0.020
C(2)–C(7)	2.052(9)	−17.28(2)	−14.38	−12.36	9.47	0.16	0.001
C(3)–C(4)	2.17(1)	−18.67(2)	−15.21	−12.78	9.33	0.19	−0.005
C(4)–C(5)	2.13(1)	−18.71(3)	−15.26	−12.47	9.02	0.22	0.044
C(5)–C(6)	2.15(1)	−19.22(3)	−15.19	−12.96	8.93	0.17	0.038
C(6)–C(7)	2.18(1)	−19.62(2)	−15.63	−13.04	9.04	0.20	0.020
C(8)–C(9)	2.14(1)	−18.82(2)	−15.16	−12.85	9.19	0.18	−0.022
C(8)–C(13)	2.192(9)	−19.96(2)	−15.43	−13.71	9.18	0.13	−0.016
C(9)–C(10)	2.18(1)	−20.16(2)	−15.56	−13.41	8.80	0.16	0.023
C(10)–C(11)	2.25(1)	−21.73(3)	−16.46	−13.94	8.68	0.18	−0.019
C(11)–C(12)	2.19(1)	−20.44(3)	−15.40	−13.61	8.57	0.13	0.049
C(12)–C(13)	2.20(1)	−20.25(2)	−15.55	−13.65	8.95	0.14	−0.024
C(14)–C(15)	2.14(1)	−19.32(2)	−15.06	−13.40	9.14	0.12	−0.024
C(14)–C(19)	2.147(9)	−18.72(2)	−14.99	−13.04	9.31	0.15	0.032
C(15)–C(16)	2.23(1)	−21.41(3)	−16.05	−13.94	8.58	0.15	0.050
C(16)–C(17)	2.14(1)	−18.96(3)	−14.95	−13.09	9.08	0.14	0.012
C(17)–C(18)	2.23(1)	−20.78(3)	−15.71	−14.07	9.01	0.12	0.021
C(18)–C(19)	2.22(1)	−19.80(2)	−15.71	−13.36	9.28	0.18	−0.021
C(20)–C(21)	2.126(9)	−18.16(2)	−14.76	−12.73	9.33	0.16	−0.027
C(20)–C(25)	2.133(9)	−18.17(2)	−14.77	−12.81	9.40	0.15	−0.001
C(21)–C(22)	2.21(1)	−20.65(2)	−15.98	−13.59	8.92	0.18	−0.001
C(22)–C(23)	2.21(1)	−20.56(3)	−15.59	−13.78	8.81	0.13	−0.043
C(23)–C(24)	2.19(1)	−20.10(3)	−15.71	−13.42	9.02	0.17	−0.031
C(24)–C(25)	2.17(1)	−20.33(2)	−15.73	−13.49	8.89	0.17	−0.006

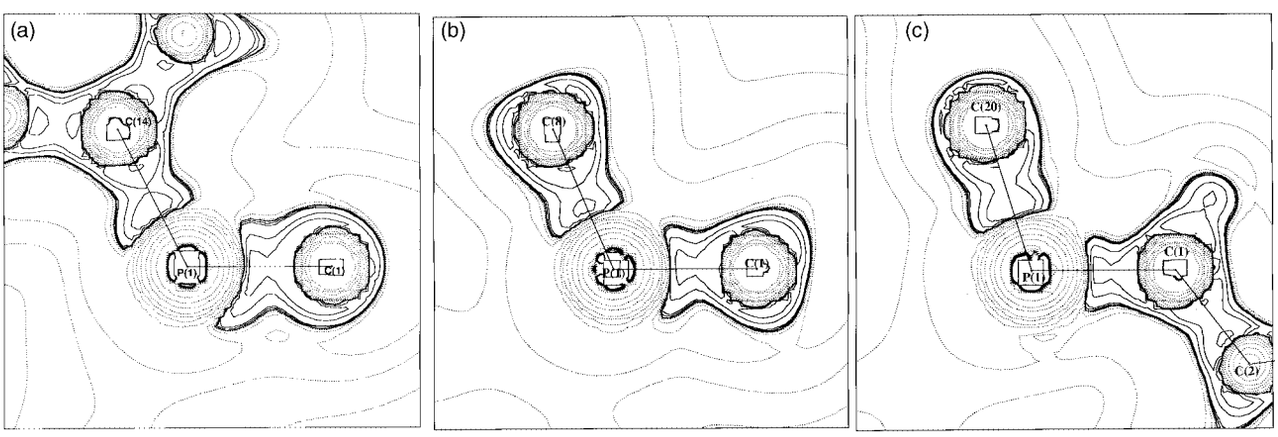

Fig. 2 The Laplacian maps in the planes C(1)P(1)C(14) (a), C(1)P(1)C(8) (b) and C(1)P(1)C(20) (c). Contours at logarithmic intervals in $-\nabla^2\rho$/e Å^{-5}.

direction is found. It seems that these shifts of the BCP positions reflect the charge transfer from the stabilising phenyl group towards the (PPh_3) fragment and show the different roles played by the Ph rings in delocalisation of the charge. High values of relative shift Δ_{ij}, indicate that the shape of the atomic basin of phosphorus deforms quite easily.

There are several short intramolecular contacts between the non-bonded atoms of the phenyl rings of molecule **1**. The analysis of charge density distribution in the regions of these close contacts reveals the presence of three bond paths with corresponding BCP (Table 4, Fig. 3). Similar bond paths corresponding to close intramolecular contacts have been found experimentally (for the first time, probably, in ref. 16) and analysed theoretically. The discussion about the interpretation of such contacts is still going on in the literature (see, for example, ref. 17 and references therein). In molecule **1** these contacts have the usual low values of total density for such

Table 4 Parameters of the CP for intra- and inter-molecular non-bonded interactions in the structure **1** (R_{ij} is the C···H distance along the bond path)

Interaction	ρ	$-\nabla^2(\rho)$	R_{ij}
Intra			
H(3)···C(8)	0.061(1)	0.708(1)	2.7094
H(21)···C(13)	0.055(2)	0.754(1)	2.6715
H(9)···C(14)	0.067(1)	1.028(1)	2.5977
Inter			
H(25)···C(7)[a]	0.041(2)	0.578(1)	2.8356
H(19)···C(25)[a]	0.054(2)	0.635(1)	2.7697
C(24)···H(10)[b]	0.039(3)	0.644(1)	2.7156
C(19)···H(23)[c]	0.040(2)	0.567(1)	2.7216

[a] $-x, 2-y, -z$. [b] $-x, 1-y, -z$. [c] $1+x, y, z$.

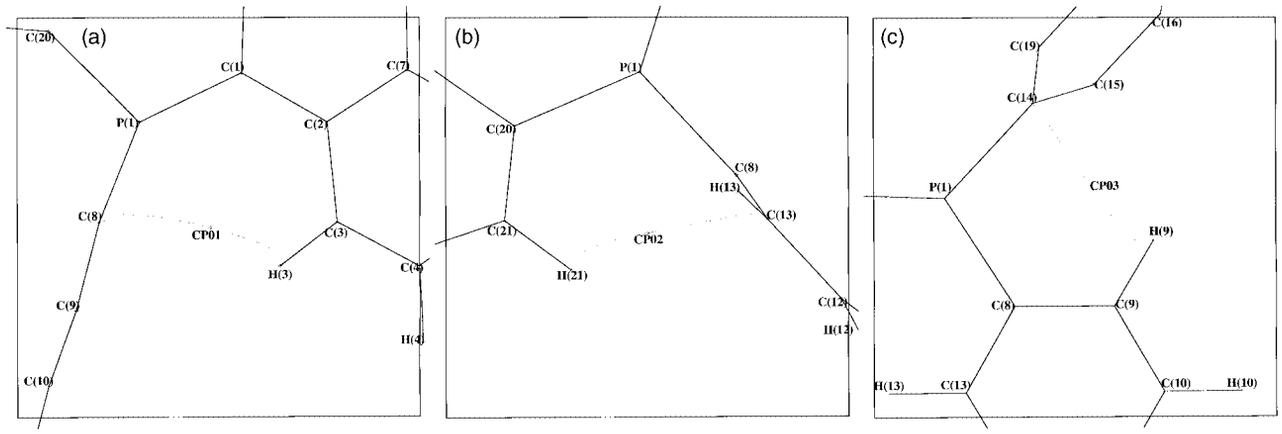

Fig. 3 Bond paths of intramolecular interactions.

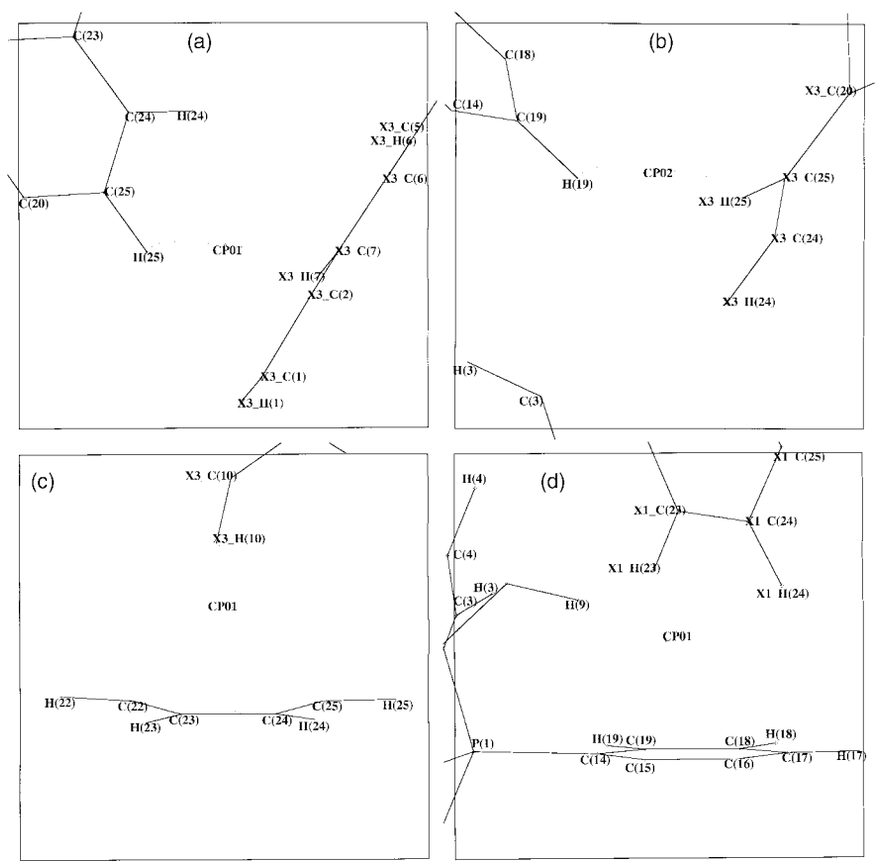

Fig. 4 Bond paths of intermolecular interactions. X indicates atoms of the molecules related to the original one by $(-x, 2 - y, -z)$ (4a, 4b), $(-x, 1 - y, z)$ (4c) and $(1 + x, y, z)$ (4d).

interactions and positive values of the Laplacian. The sharp bend of the bond paths near hydrogen atoms is a typical feature of short contacts where the C–H vector is not pointed straight toward the acceptor atom. This bend was observed, for example, in theoretical calculations of the topology of C–H···O interactions.[18] Corresponding ring critical points were also found for all three intramolecular interactions.

According to the conventional X-ray structure analysis[4] the packing of molecules in the crystal is determined by the pairs of C(25)–H(25)···C(1)′ interactions, which link molecules in centrosymmetrical dimers. However, all our attempts to find any signs of these interactions on the basis of analysis of the experimental charge density distribution failed. In fact the molecules are linked in these previously described dimers but in a different way. The centrosymmetrical dimer is held together by two pairs of bond paths, which correspond to the C(25)–H(25)···C(7)′ and C(19)–H(19)···C(25)′ interactions (Table 4, Fig. 4). This pair of contacts has longer C···H distances than those of C(25)–H(25)···C(1)′, and a not so (seemingly) favorable direction of the C–H bond, but the C···C distances are smaller. Additional interactions, also listed in Table 4, connect the molecules in a three-dimensional network. The parameters of BCP and the geometry of bond paths of these contacts are similar to those for intramolecular non-bonded contacts. One exception is the C(10)–H(10)···C(24) contact. The bond path of the interaction is directed towards the middle of the C(23)–C(24) bond and then makes a sharp turn to C(24). A similar shape of the bond path was obtained from *ab initio* calculations of the systems with X–H···π bonds.[19] The "ideal" atomic interaction line for X–H···π interaction is terminated in the middle of the multiple bond. However, it creates a so-called conflict structure and in the real crystal the bond path is switched to the nearest nuclear attractor. Therefore we have to regard the contact as a C(10)–H(10)···π interaction.

Conclusions

The topological analysis of the experimentally determined charge density distribution in semi-stabilized ylide **1** revealed features of the fine electron structure of the molecule. The multiple character and high ionicity of the ylide bond have been observed and a different role for the phenyl groups in the PPh_3 fragment has been shown. It was shown that the shortest distance between C and H atoms in neighboring molecules does not necessarily imply the presence of a C–H $\cdots$ C interaction between these atoms. This work is another illustration of the fact that charge density studies provide unique information about the molecular and crystal structure.

Acknowledgements

Authors are grateful for financial support by the Engineering and Physical Sciences Research Council (UK).

References

1 D. G. Gilheany, *Chem. Rev.*, 1994, **94**, 1339.
2 H. Schmidbaur, J. Jeong, A. Schier, D. Graf, D. L. Wilkinson and G. Muller, *New J. Chem.*, 1989, **13**, 341.
3 R. F. W. Bader, *Atoms in Molecules – a quantum theory*, 1990, Clarendon Press, Oxford.
4 A. S. Batsanov, M. G. Davidson, J. A. K. Howard, S. Lamb and C. Lustig, *Chem. Commun.*, 1996, 1791.
5 R Flaig, T. Koritsanszky, D. Zobel and P. Luger, *J. Am. Chem. Soc.*, 1998, **120**, 2227.
6 SAINT, Version 5.00, Bruker AXS, Madison, USA, 1998.
7 R. Blessing, *J. Appl. Crystallogr.*, 1997, **30**, 421 and references therein.
8 T. Koritsanszky, S. Howard, T. Richter, P. R. M. Mallinson, Z. Su and N. Hansen, *XD. A Computer Program Package for Multipole Refinement and Analysis of Electron Densities from Diffraction Data*, Berlin, Cardiff, Glasgow, Buffalo, Nancy, 1994.
9 P. Coppens, *X-Ray Charge Densities and Chemical Bonding*, Oxford University Press, 1997.
10 F. H. Allen, O. Kennard, D. G. Watson, L. Brammer, A. G. Orpen and R. Taylor, *J. Chem. Soc.*, *Perkin Trans. 2*, 1987, Suppl. 1.
11 G. R. Moss, M. Souhassou, E. Espinosa, C. Lecomte and R. H. Blessing, *Acta Crystallogr.*, *Sect. B*, 1995, **51**, 650.
12 F. L. Hirshfeld, *Acta Crystallogr.*, 1976, **32**, 239.
13 R. F. Stewart, in *The Application of Charge Density Research to Chemistry and Drug Design*, eds. G. A. Jeffrey and J. F. Piniella, NATO ASI Series, Vol. B250, 1991, Plenum Press, NY, pp. 63–101.
14 N. Sandblom, T. Ziegler and T. Chivers, *Can. J. Chem.*, 1996, **74**, 2363.
15 D. S. Yufit, P. R. Mallinson, K. W. Muir, S. I. Kozhushkov and A. deMeijere, *Acta Crystallogr.*, *Sect. B*, 1996, **52**, 668.
16 R. Destro and F. Merati, *Acta Crystallogr.*, *Sect. B*, 1995, **51**, 559.
17 R. F. W. Bader, *J. Phys. Chem. A*, 1998, **102**, N 37, 7314.
18 U. Koch and P. L. A. Popelier, *J. Phys. Chem.*, 1995, **99**, 9747.
19 T. H. Tang and Y. P. Cui, *Can. J. Chem.*, 1996, **74**, 1162.

Paper a908099f